

First identification and compositional study of brown aerinite directly on polished thin-sections by synchrotron through-the-substrate microdiffraction

ANNA CRESPI¹, ORIOL VALLCORBA², IGORS ŠICS² and JORDI RIUS^{1*}

¹Institut de Ciència de Materials de Barcelona, CSIC, Campus de la UAB, 08193 Bellaterra, Catalonia, Spain

²ALBA Synchrotron Light Source (CELLS), 08920 Cerdanyola del Vallès, Barcelona, Spain

*Corresponding author, e-mail: jordi.rius@icmab.es

Abstract: A brown variety of the fibrous chain silicate aerinite has been identified by synchrotron *through-the-substrate* (*tts*) microdiffraction [$a = 16.937(2)$, $c = 5.223(1)$ Å, $V = 1297.5(3)$ Å³, $P3c1$, illuminated sample volume = $15 \times 15 \times 30$ μm³]. The small zone containing the brown submicrometric fibers was detected next to a pale-blue aerinite region during the inspection of a polished thin-section of a specimen from Tartareu (Catalonia, Spain). Compared to pale-blue aerinite, brown aerinite is Si poorer, Fe richer and its lower Ca content is compensated by a Mn increase. By using the total number of electrons at sites M1a, M1b, M2, M3, T1a and T1b supplied by the Rietveld refinement, the atomic proportions derived from the electron microprobe analysis (EMPA) of the small brown zone could be scaled to $\text{Si}_{11.7}\text{Al}_{5.8}\text{Fe}_{4.6}\text{Mg}_{0.9}\text{Mn}_{2.0}\text{Ca}_{2.8}\text{Na}_{0.1}\text{K}_{0.1}$. This gives a total of 28 atoms which implies that the 28 cationic sites of the aerinite crystal structure are fully occupied. In this refinement, the carbonate ions, centered along a ternary axis, converged to a staggered stacking with 0.94(1) occupancy. The atomic distribution of brown aerinite has been studied by combining the refined scattering power values at the cationic sites with the EMPA results. According to this study, one important difference with respect to blue aerinite is the presence at sites M2 and M3 of large percentages of (Fe, Mn) atoms, i.e. ~30% and ~50%, respectively. This work constitutes an example of the utility of the *tts*-μXRD technique when complex rocks with mineral components showing significant compositional differences need to be characterized.

Key-words: aerinite; *tts*-μXRD, synchrotron; polished thin section; Rietveld refinement; aluminosilicate; cationic distribution

1. Introduction

Aerinite is a trigonal fibrous silicate mineral first described by Von Lasaulx (1876) and later confirmed as a new mineral species by Azambre & Monchoux (1988). Its crystal structure was solved from synchrotron powder diffraction data by Rius, Elkaim, Torrelles (2004). Historically, aerinite is a blue pigment used in many romanian paintings, mainly in the Pyrenean region, between the XI-XIV centuries (Palet & de Andres, 1992). The blue color varies from dark to pale-blue. By using Mössbauer spectroscopy, the blue tonality could be ascribed to the amount of mixed valence iron (Tura, Castellar, Font-Altaba, Marsal, Morer, Plana, Traveria 1988), a point which was later confirmed by applying powder X-ray diffractometry and Mössbauer spectrometry to a specimen from Tartareu (Catalonia, Spain) containing pale-blue aerinite (Rius, Crespi, Roig, Melgarejo, 2009). However, one double question still remains open: 'Must aerinite be always blue?' or 'Is it always blue simply because it can only be clearly identified when it is blue?'. To shed light on this point the synchrotron through-the-substrate microdiffraction (*tts- μ XRD*) technique (Rius, Labrador, Crespi, Frontera, Vallcorba, Melgarejo, 2011) was applied to a polished thin-section of the Tartareu specimen. This technique allows visualizing the thin-section (eventually under polarized light) and at the same time acquiring diffraction patterns at target points previously identified either by scanning electron microscopy - energy dispersive X-ray spectroscopy (SEM-EDS), electron microprobe analyses (EMPA) or backscattered electrons (BSE) images. In the course of the optical inspection of the Tartareu thin-section, a region formed by brown submicrometric fibers was found next to pale-blue aerinite (Fig. 1 and 2). The SEM-EDS analysis of the brown region suggested an aerinite-related composition with somewhat higher Fe content, and with Mn partially replacing Ca (Table 1). Due to the significant compositional difference, synchrotron *tts- μ XRD* data were first collected to verify that the brown fibers were indeed aerinite. The diffraction study was complemented with accurate EMPA measurements.

FIGURE 1

FIGURE 2

2. Experimental procedures

2.1. Chemical analysis

The equipment used was a JEOL JXA-8230. From the two modes of analyzing X-rays in EMPA, i.e. by energy dispersive spectrometry (EDS) or with a wavelength dispersive spectrometer (WDS), here the EDS mode was preferred to minimize the damage caused by electronic beam damage [as compared to WDS the current in EDS mode is lower (1 nA vs. 6-10 nA)]. When the

matrix effect is corrected and if there is no peak overlap in the EDS spectrum, EDS results are as accurate as WDS results. The operation conditions were: voltage 12 KV, probe current 1 nA, peak counting time 60s, beam diameter of 10 μm . Standards used: albite (Na), diopside (Si), wollastonite (Ca), orthoclase (K), Fe_2O_3 (Fe), rhodonite (Mn), corundum (Al), periclase (Mg). To circumvent any alteration due to sample damage, the chemical composition of the brown region was determined from EMPA data taken at 27 points around the target point of the previously performed *tts*- μXRD experiment (Table 1, column a). For comparison purposes, Table 1 also includes the EMP analyses of pale-blue aerinite next to the brown region (column b) and of pale-blue aerinite fibers taken from the external part of the specimen (column c; Rius *et al.*, 2009). In this last case, the difference to 100 (~17%) corresponds to the amount of water molecules and carbonate ions. Finally, the chemical analyses were complemented by element distribution maps (Si, Al, Fe, Ca and Mg; Fig. 3).

TABLE 1
FIGURE 3

2.2. Synchrotron *tts*- μXRD data collection and processing

Diffraction data were collected at the microdiffraction/high-pressure station of the MSPD beamline (ALBA Synchrotron, Barcelona, Spain) (Fauth *et al.*, 2013). It is equipped with Kirkpatrick–Baez mirrors providing a monochromatic focused beam of 15 x 15 μm^2 (full width at half maximum) and a Rayonix SX165 CCD detector (round active area of 165 mm diameter, frame size 2048 x 2048 pixels, 79 μm pixel size, dynamic range 16 bit). The used beam energy was 29.2 keV ($\lambda = 0.4246 \text{ \AA}$), as determined from the Sn absorption K edge. The sample-to-detector distance and the beam center position were calibrated using the d2Dplot software (Vallcorba & Rius, 2019) with LaB_6 as calibrant. The sample was placed on a xyz stage with the thin-section (~30 μm thickness) facing the detector and mounted on a 1 mm thick glass-substrate. The measurement point was selected in the middle of the brown Mn-bearing region with the help of an on-axis ultrazoom microvisualization system (equipped with polarized light). The 2D diffraction pattern was obtained by rotating the sample $\pm 7.5^\circ$ around the vertical tilt axis (30 s). To remove the most of the glass-substrate contribution, an additional 2D pattern of the glass-substrate was collected under the same conditions. The ‘powder’ diffraction pattern of the brown zone was obtained by circularly averaging the corresponding difference 2D pattern.

FIGURE 4

3. The aerinite crystal structure

3.1 Description and atom labeling

As can be seen in the schematic view of the unit cell of pale-blue aerinite (Fig. 4), the aerinite crystal structure is formed by two-symmetry independent triads of pyroxene-like chains pointing inwards to accommodate tri- and divalent cations giving rise to two similar symmetry-unrelated columns of face-sharing octahedra (identified by the a and b suffixes). Sites M1a and M1b are at the centers of the face-sharing octahedra. The T1a site is occupied by the tetrahedrally coordinated T1a atoms (Si, Al) of the pyroxene chains with O1a, O2a and O3a being, respectively, the apical, lateral and shared O ligands. Each columnar unit is formed by six T1, 18 O and two M1 atoms. The two symmetry-independent columnar units are centered along the ternary axes at (0, 0, z) and (1/3, 2/3, z) and joined together by slabs of corner-sharing octahedra centered at the M2 and M3 sites. In blue aerinite, site M2 is filled with Al³⁺ and a small amount of Mg²⁺ ions; site M3 hosts the large Ca²⁺ ion and some vacancies. The Al³⁺ ions at M2 are coordinated by four hydroxyl ions [O4a (2x) and O4b (2x)] and by the two O2a and O2b ligands. In its turn, the Ca²⁺ ion at site M3 is linked to atoms O4a, O4b, O2a, O2b and to the O5 and O6 of water molecules. The respective number of non-carbonate O atoms is 60, i.e. 36 framework O atoms + 12 hydroxyl ions + 12 water molecules, which represent a total of 84 negative formal charges. The small carbonate anions are along the ternary axis at (2/3, 1/3, z) (Fig. 4). One characteristic of blue aerinite is the reversible phase transition around 250 °C in which CO₂ and water are released (Besteiro, Lago-San José, Pocoví, Bastida, Amigó, Moliner, 1985; Azambre & Monchoux, 1988).

3.2 Stabilization of mixed valence iron in blue aerinite

In blue aerinite, the M1a and/or M1b sites (generically M1) host Fe atoms in mixed valence state (Tura *et al.*, 1988; Rius *et al.*, 2009). Since atom O1 is linked to two M1 atoms and to one T1 atom (Si), it can only reach its formal charge if site M1 is occupied by a trivalent cation like Fe³⁺. However, if mixed-valence Fe atoms are present, e.g. Fe^{2.5+}, atom O1 still needs 0.17 valence units (vu) to compensate for the missing cationic charge. As already described in Rius *et al.* (2004), the O4 hydroxyl ion plays a key role in this compensation. Since it forms two strong bonds with Al atoms at M2 (2 x ~0.5 vu) and a weaker one with Ca atoms, its total bond valence sum is ~2.17 vu (proton contribution included). The exceeding ~0.17 vu are donated by atom O4 to atom O1 *via* a hydrogen bond.

FIGURE 5

4. Results

4.1 Identification of the brown fibers

The close similarity between the ‘powder’ diffraction pattern of the brown fibers and the powder pattern of pale-blue aerinite [measured in a capillary of $\varnothing = 1\text{mm}$; Rius *et al.* (2009)] confirms that the brown fibers correspond to aerinite (Fig. 5). The value of the a parameter for brown aerinite after the Rietveld refinement is significantly greater than for pale-blue aerinite and much larger than for dark-blue Fe-poor aerinite, namely 16.937(2), 16.9161(1) (Rius *et al.*, 2009) and 16.8820(9) (Rius *et al.*, 2004), respectively.

4.2 The Rietveld refinement

The *tts*- μ XRD ‘powder’ data used in the Rietveld refinement correspond to an irradiated sample volume of approximately $15 \times 15 \times 30 \mu\text{m}^3$. The average chemical composition, estimated from 27 EMPA measurement points, is given in Table 1. The Rietveld refinement was performed with the atomic coordinates of pale-blue aerinite as starting model. To minimize the bias caused by inaccurate target values, only the T1a – O1a, T1b – O1b and C1- O7 distance restraints were introduced. Si atoms were placed at the T1a and T1b sites (Si and Al atoms are undistinguishable by powder X-ray diffraction). Only the occupancies of Al atoms at M2, of Ca atoms at M3 and of the carbonate ions were refined. The resulting scattering powers (s.p.’s) in electrons (e) are 13(2) at M1a; 27(2) at M1b; 17.3(7) at M2; 21.1(5) at M3. The carbonate ions converged to a staggered stacking with 0.94(1) occupancy. The refined atomic coordinates are listed in Table 2. The refined M1a-O1a and M1b-O1b bond lengths are 2.1(1) and 1.9(1), respectively. For the octahedral M2 site, the refinement gives $\langle \text{M2} - \text{O} \rangle = 2.17 \text{ \AA} (6x)$; $\langle \text{M2} - \text{O4a} \rangle = 1.95 \text{ \AA} (2x)$ and $\langle \text{M2} - \text{O4b} \rangle = 2.29 \text{ \AA} (2x)$. By adding the total number of electrons at the sites M1a, M1b, M2, M3, T1a and T1b (478.1 e), the atomic proportions from EMPA could be scaled to $\text{Si}_{11.72}\text{Al}_{5.80}\text{Fe}_{4.64}\text{Mg}_{0.89}\text{Mn}_{1.96}\text{Ca}_{2.80}\text{Na}_{0.10}\text{K}_{0.09}$. This gives a total of 28.0 atoms, exactly the number of cationic sites in the unit cell. The R -values at the end of the refinement are $R_{\text{wp}} = 0.046$; $R_{\text{p}} = 0.033$ (Langford & Louër, 1996) with $\chi = R_{\text{wp}}/R_{\text{model-free}} = 1.24$ (Fig. 6). The Rietveld refinement was performed with a version of RIBOLS18 (Rius, 2012) adapted to *tts*- μ XRD data: 2θ range = $1 - 22^\circ$; number data points = 879; number contributing reflections = 331; peak range in FWHM = 20; number profile/structural parameters = 6/50;; profile function: Thompson, Cox, Hastings (1987) with $w_{\text{L}} = Y / \cos\theta$ [deg.] and $w_{\text{G}}^2 = U$ [deg.²] where $Y = 0.036(2)$ and $U = 0.0027(2)$; zero shift = $-0.0127 (5)^\circ$; weighting factor = $1/y_0$; excluded (aerinite-free) regions in 2θ : from 1.00 to 1.41, 2.05 to 2.68, 3.44 to 4.25, 4.50 to 4.80, 5.12 to 5.35, 6.78 to 7.11, 7.71 to 8.18 $^\circ$.

TABLE 2
FIGURE 6

5. Discussion and conclusions

Table 2 shows the clear atomic correspondence between brown and pale-blue aerinite, thus confirming that both compounds are isostructural. It can be seen that the O5, O6 and O4b atoms have larger positional discrepancies. The O5 and O6 atoms form a cylindrical surface of close-packed O atoms with its inner space filled with the carbonate ions staggered along the ternary axis at $(2/3, 1/3, z)$. The presence of sulfate anions in brown aerinite can be excluded, since no S was detected. This is in agreement with the high occupancy of the carbonate anion, 0.94(1). Regarding the pyroxene-like chains, there are only 11.7 Si atoms according to the scaled EMPA results. This means that the T1a and/or T1b sites are slightly Si deficient with 0.3 Al atoms being the preferential candidate to complete them. The analysis of the distribution of the Al, Mg, Fe, Mn and Ca atoms among the M1a, M1b, M2 and M3 sites is simplified by the fact that i. all metal sites are fully occupied; ii. the large Ca^{2+} ions occupy the M3 site in aerinite; iii. the four remaining atom types form two groups, (Al, Mg) and (Fe, Mn), each one with very similar scattering powers but with marked contrast between them:

5.1. M1a and M1b sites

The refined s.p. value at M1a is 13(2) e; consequently, only (Al, Mg) atoms can occupy this site. Similarly, for M1b, the refined s.p. value is 27(2) e, so that only (Fe, Mn) atoms can enter this site.

5.2 M2 site

The refined s.p. value at M2 is 17.3(7) e which falls between 12-13 and 25-26 e, so that this site must host mixed (Al, Mg) and (Fe, Mn) atoms. The approximate fraction of (Fe, Mn) atoms, $x_{\text{Fe,Mn}}$ = 0.34, is obtained from equation $17.3 = 12.9 \cdot (1 - x_{\text{Fe,Mn}}) + 25.7 x_{\text{Fe,Mn}}$ [12.9 and 25.7 are the average atomic numbers of (Al,Mg) and (Fe,Mn)]. In pale-blue aerinite, the coordination of the Al atoms at site M2 is a regular octahedron [$\langle\text{M2-O}\rangle$ bond length = 1.92(6) Å]. In contrast, the Rietveld refinement of brown aerinite indicates that the coordination of the M2 atom is a distorted octahedron with a clear asymmetry between the $\langle\text{M2-O4a}\rangle$ and $\langle\text{M2-O4b}\rangle$ bond lengths. All attempts to increase the octahedron regularity through additional distance restraints ended with a significant R-value increase, thus confirming the distortion. This could be related to the presence of some water molecules as M2 ligands.

5.3. M3 site

The refined s.p. value at this site is 21.1(5) e. The 2.8 Ca atoms occupying this site contribute with 9.3 e to the refined s.p. value. Since the site must be fully occupied, the s.p. difference (11.8 e) corresponds to atoms with a s.p. close to 22 e, e.g. (Mn, Fe) atoms. This is also in agreement with the clear negative correlation between Ca and Mn found in the element distribution maps of

aerinite. Since the size difference between Ca^{2+} and $\text{Mn}^{2+}/\text{Fe}^{2+}$ ions is large, the M3 site should tolerate a splitting which was confirmed by an additional Rietveld refinement, i.e. site M3' at [.355(4), 0.343(2), 0.4869(4)] and site M3'' at [.351(5), 0.308(4), 0.4831(4)] with respective s.p. values being 14(2) and 8(2) e.

The result of the atomic distribution analysis is summarized in Table 3. Regarding the atomic distribution the two principal differences between brown and blue aerinite are: i. the partial substitution of Al atoms by (Fe,Mn) ones at site M2 (~30%); ii. the partial substitution of Ca atoms by (Mn,Fe) ones at site M3 (~50%).

TABLE 3

This study constitutes an example of the utility of the *tts- μ XRD* technique when complex rocks with mineral components showing large compositional differences need to be characterized. In such cases the complementarity of SEM-EDS, EMPA and local *tts- μ XRD* experiments is most helpful in unravelling complicate cationic distributions. In the present case, detailed information on the atomic distribution of brown aerinite has been obtained by combining these techniques. Especially important were the refined scattering power values, since they are reliable even with diffraction data of moderate quality. Undoubtedly, a source of progress for the complete characterization of brown aerinite would be the determination of the oxidation states of the Fe atoms. A μ -XAS experiment on the same polished thin section could be helpful in this point.

Acknowledgements: This work was carried out in the frame of the Materials Science Doctorate of the 'Universitat Autònoma de Barcelona'. Financial support of projects MAT2015-67593-P, Severo Ochoa" SEV-2015-0496 and RTI2018-098537-B-C21) of MINECO & FEDER is acknowledged. Thanks are also due to the ALBA synchrotron (Barcelona, Spain) for beamtime (experiment 2017032195), to the 'Centres Científics i Tecnològics de la Universitat de Barcelona' for the EMP analyses, to the 'Lab. de Preparació de Làmines Primes, Dpt. de Geologia, U. Autònoma de Barcelona' for the polished thin-section preparation and, finally, to Mr. Joan Font for donating the specimen.

References

- Azambre, B. & Monchoux, P. (1988): Precisions mineralogiques sur l'aerinite: nouvelle occurrence a Saint-Pandelon (Landes, France). *Bull. Mineral.*, **111**, 39-47.
- Besteiro, J., Lago-San José, M., Pocoví, A., Bastida, J., Amigó, J.M., Moliner, R. (1985) Nuevos datos mineralógicos sobre un inclasificado aluminosilicato, aerinita, y consideraciones sobre su atribución al grupo de las Ceolitas. *Acta Geológica Hispánica*, **20**, 257-266.
- Fauth, F., Peral, I., Popescu, C. & Knapp, M. (2013): The new Materials Science and Powder diffraction beamline at ALBA synchrotron. *Powder Diffraction*, **28**(S2), S360-S370.
- Langford, J.I. & Louër, D. (1996): Powder Diffraction. *Rep. Prog. Phys.*, **59**, 131-234.
- Momma, K., Izumi, F. (2011): VESTA 3 for three-dimensional visualization of crystal, volumetric and morphology data. *J. Appl. Crystallogr.*, **44**, 1272-1276.
- Palet, A. & de Andres, J. (1992): The identification of aerinite as a blue pigment in the Romanesque frescoes of the Pyrenean region. *Studies in Conservation*, **37**, 132-136.
- Rius, J., Elkaim, E., Torrelles, X. (2004): Structure determination of the blue mineral pigment aerinite from synchrotron powder diffraction data: The solution of an old riddle. *Eur. J. Mineral.*, **16**, 127-134.
- Rius, J., Crespi, A., Roig, A., Melgarejo, J.C. (2009): Crystal-structure refinement of Fe³⁺-rich aerinite from synchrotron powder diffraction and Mo'ssbauer data. *Eur. J. Mineral.*, **21**, 233-240.
- Rius, J., Labrador, A., Crespi, A., Frontera, C., Vallcorba, O. & Melgarejo, J. C. (2011): Capabilities of through-the-substrate microdiffraction: Application of Patterson-function direct methods to synchrotron data from polished thin sections. *J. Synchrotron Rad.* **18**, 891-898.
- Rius, J. (2012): RIBOLS18: A computer program for restrained Rietveld refinement. Institut de Ciencia de Materials de Barcelona (CSIC), Barcelona (Spain).
- Thompson, P., Cox, D.E., Hastings, J.B. (1987): Rietveld refinement of Debye-Scherrer Synchrotron X-ray data from Al₂O₃. *J. Appl. Cryst.*, **20**, 79-83.
- Tura, J.M., Castellar, M.D., Font-Altaba, M., Marsal, M., Morer, A., Plana, F., Traveria, A. (1988): Study of the blue pigments of the mural paintings of the Vall de Boí (Catalonia, 11th - 12th century) by means of SEM/EDXA. *Beitr. Elektronenmikroskop Direktabb. Oberfl.*, **21**, 298-303.
- Vallcorba, O., Rius, J. (2019): d2Dplot: 2D X-ray diffraction data processing and analysis for through-the-substrate microdiffraction. *J. Appl. Cryst.*, **52**, 478-484.
- Von Lasaulx, A. (1876): Äerinit, ein neues Mineral. *N. Jb. Mineral.*, 175 and 352-358.

Table 1. Electron-microprobe analyses of the Tartareu specimen (wt%) corresponding to: (a) brown ‘aerinite’ in the thin-section (average of 27 points with standard deviation in parentheses) (Fig. 1); (b) pale-blue aerinite in the thin-section (Fig. 1); (c) a massive fiber bundle of pale-blue aerinite from the external part of the specimen (Rius *et al.*, 2009); (d) column (a) given as wt% of the cations.

oxide	a	b	c	d
SiO ₂	28.4 (6)	32.1 (4)	40.32	13.27
Al ₂ O ₃	11.9 (3)	12.1 (2)	15.38	6.31
MgO	1.44 (4)	0.81 (6)	1.82	0.87
FeO	13.5 (4)	10.5 (3)	12.48	10.45
CaO	6.3 (4)	10.1 (2)	13.07	4.52
MnO	5.6 (3)	0.21 (6)	0.03	4.34
Na ₂ O	0.12 (2)	0.39 (6)	0.18	0.09
K ₂ O	0.17 (2)	0.09 (3)	0.02	0.15
Σ	67.43	66.30	83.30	40.00

Table 2. Fractional coordinates of brown aerinite [$a = 16.936(2)$, $c = 5.223(1)$] and published ones of pale-blue aerinite (external part) [$a = 16.9161(1)$, $c = 5.2289(1)$] with s.u.s given in parentheses. (Respective overall B values are 1.5(2) and 0.8(2) Å²; refined scattering power values of metal sites of brown aerinite are given in Section 4.2). To facilitate the comparison between both sets, the z (M1b) coordinates of the two aerinite varieties were made coincident. The Rietveld refinement of brown aerinite only used the T1a-O1a (4x), T1b-O1b (4x) and C1-O7, O7...O7 (2x) distance restraints.

Atom	Brown aerinite			Pale - blue aerinite		
	x	y	z	x	y	z
M1a	0	0	0.1032(4)	0	0	0.0354(5)
M1b	1/3	2/3	0.8455 ^[*]	1/3	2/3	0.8455
M2	0.200(3)	0.325(4)	0.9335(4)	0.2134(5)	0.3336	0.9708
M3	0.341(2)	0.340(3)	0.4853(4)	0.3325(4)	0.3383(6)	0.4937
T1a	0.188(3)	0.140(3)	0.7416(4)	0.2045(5)	0.1479(7)	0.797(2)
T1b	0.392(2)	0.515(3)	0.0888(4)	0.3919(6)	0.5207(7)	0.119(2)
O1a	0.086(4)	0.084(6)	0.8532(4)	0.0912(6)	0.0890(6)	0.7854(5)
O2a	0.262(5)	0.242(4)	0.8214(4)	0.2434(9)	0.2522(7)	0.830(3)
O3a	0.221(5)	0.115(5)	0.4838(4)	0.237(1)	0.130(1)	0.518(3)
O1b	0.337(7)	0.569(7)	0.0955 ^[*]	0.336(9)	0.5772(5)	0.0955(5)
O2b	0.320(5)	0.416(3)	0.1986(4)	0.335(1)	0.4131(8)	0.101(3)
O3b	0.462(5)	0.555(6)	0.3214(4)	0.443(1)	0.539(1)	0.389(3)
O4a	0.197(6)	0.283(5)	0.3149(4)	0.171(1)	0.269(1)	0.298(3)
O4b	0.247(5)	0.433(6)	0.5564(4)	0.239(1)	0.397(1)	0.663(2)
O5	0.479(5)	0.392(6)	0.5876(4)	0.496(8)	0.386(1)	0.721(3)
O6	0.427(6)	0.256(6)	0.0903(4)	0.401(1)	0.298(1)	0.206(4)
O7	0.5949(4)	0.2526(9)	0.0826(4)	0.578(2)	0.288(3)	0.165(5)
C1	2/3	1/3	0.0826(4)	2/3	1/3	0.12(1)

^[*] = fixed to define the origin along c

Table 3. Brown aerinite: Atomic distribution derived from EMPA and *tts*- μ XRD data. Due to their similar atomic numbers the Al and Mg atoms as well as the Fe and Mn atoms have been grouped with respective average atomic numbers equal to 12.9 and 25.7 e (used to calculate the scattering power, s.p. in electrons).

Atom/s	N. of atoms EMPA	Atomic distribution				
		T1a+T1b	M1a	M1b	M2	M3
Si	11.72	11.72				
Al, Mg	5.80 + 0.89	0.28	2		4.41	
Fe, Mn	4.64 + 1.96			2	1.59	3.01
Ca	2.80					2.80
Na	0.10					0.10
K	0.09					0.09
Multiplicity		6 + 6	2	2	6	6
s.p. (calc.)		14.0	12.9	25.7	16.3	22.6
s.p. (ref.)		14	13(2)	27(2)	17.3(7)	21.1(5)

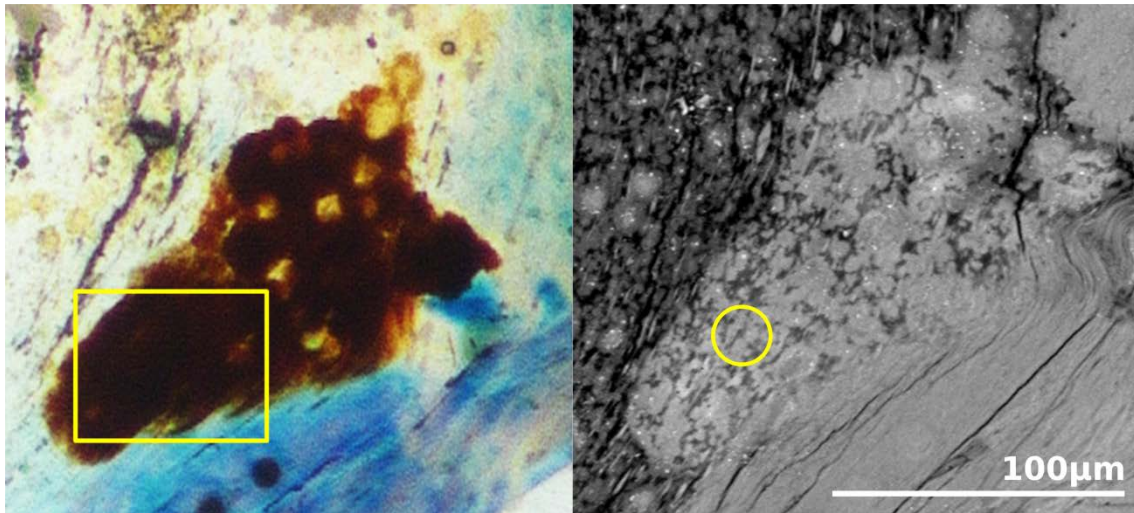


Fig. 1. (left) Photomicrograph under transmitted light of a zone of the polished thin section containing, in the middle, brown aerinite (points analysed by EMPA lie inside the yellow frame) and, in the right bottom corner of the image, pale-blue aerinite; (right) BSE image of the same zone (the yellow circumference indicates the area measured by *tts-μXRD*). The specimen comes from Tartareu.

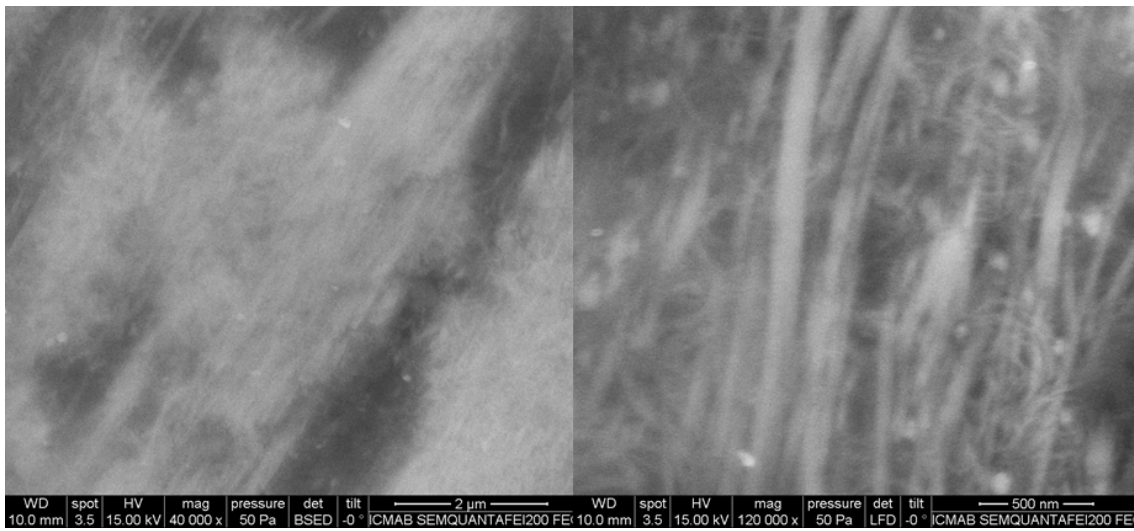


Fig. 2. BSE (left) and secondary electron SEM (right) images of the micrometric bundles of brown aerinite fibers at two different magnifications.

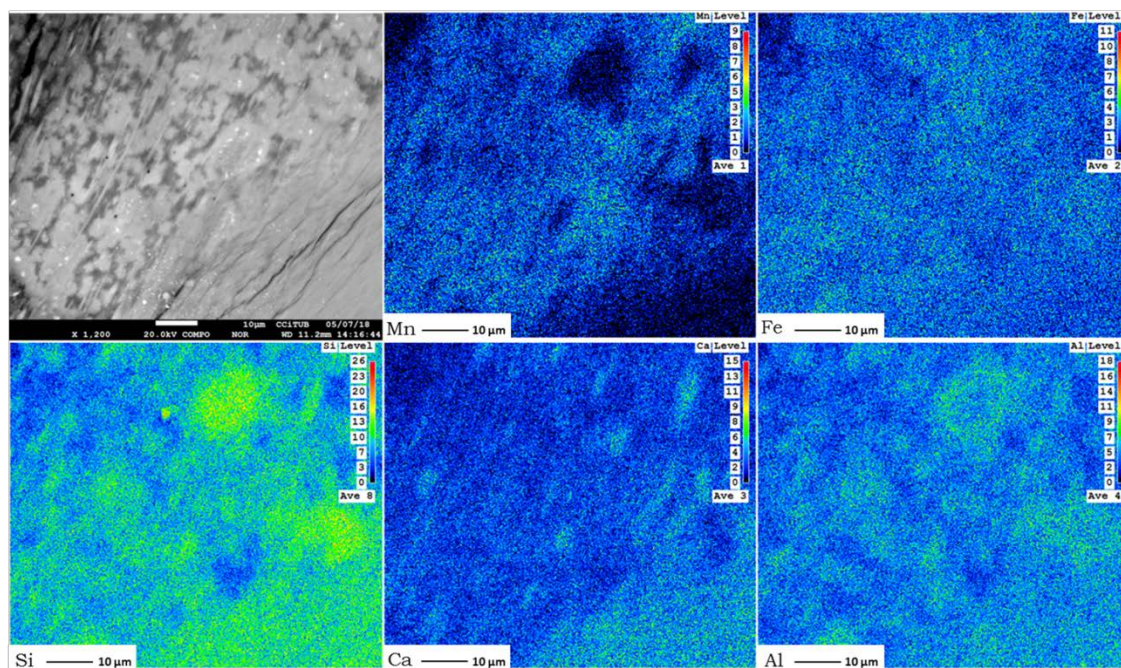


Fig. 3. Element distribution maps of the region shown in the BSE image (yellow frame in Fig 1a). The negative correlation between Mn and Ca outlines the brown and pale-blue aerinite regions. A positive correlation between the chemical elements Ca and Si is also observed.

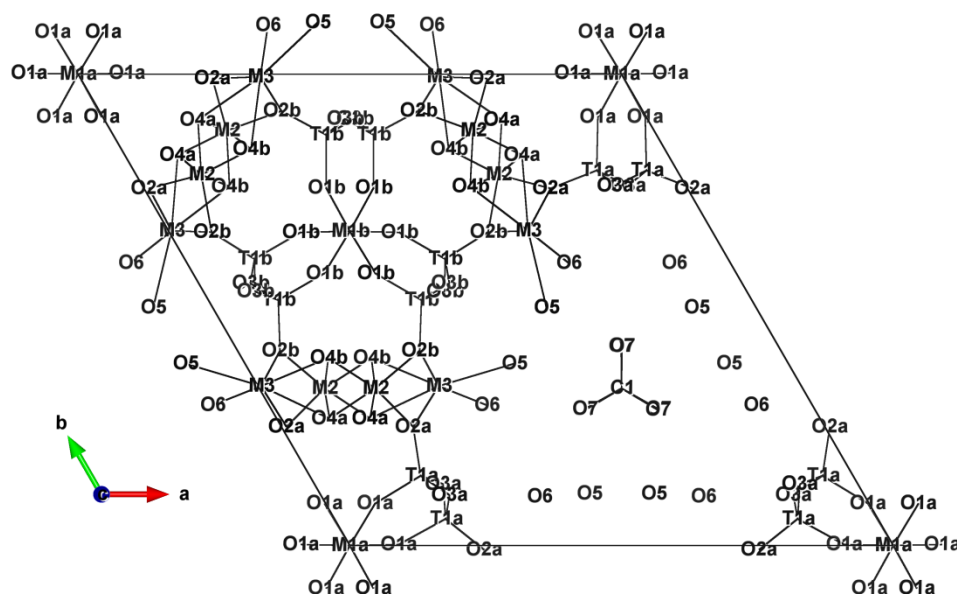


Fig. 4. Schematic view along c of the unit cell of pale-blue aerinite with atom labeling (Rius *et al.*, 2009). The columnar units are joined by structural units formed by slabs of corner-sharing octahedra of M2 and M3 atoms. The carbonate ions are centered along the ternary axis at $(2/3, 1/3, z)$. Plot created with VESTA (Momma & Izumi, 2011).

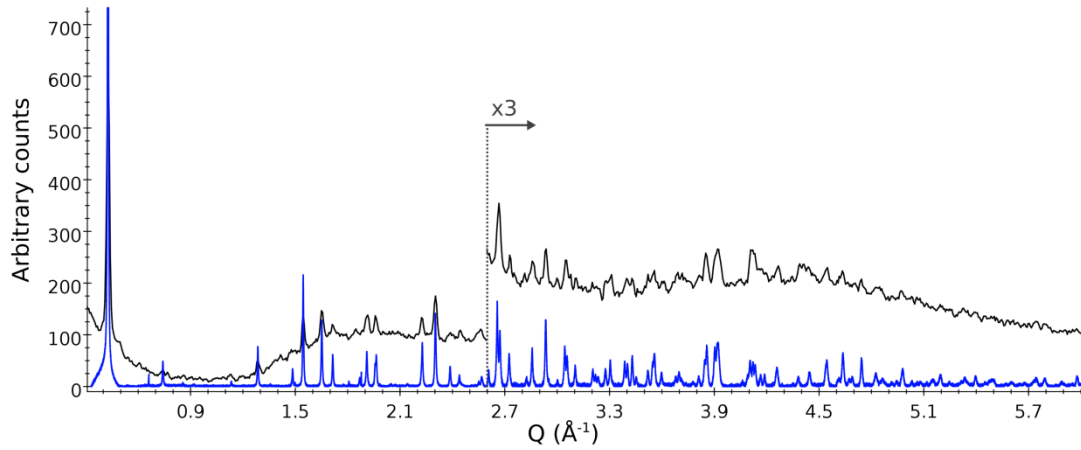


Fig. 5. ‘Powder’ diffraction pattern of brown aerinite (with some residual glass-substrate contribution) obtained by circularly averaging 2D *tts*- μ XRD images; (below, blue pattern) rescaled powder pattern of pale-blue aerinite fibers from the external part of the same specimen (sample in a 1mm \varnothing capillary; $\lambda=0.5000\text{\AA}$; Rius *et al.*, 2009). Their coincidence confirms that the brown fibers correspond to the aerinite structure type.

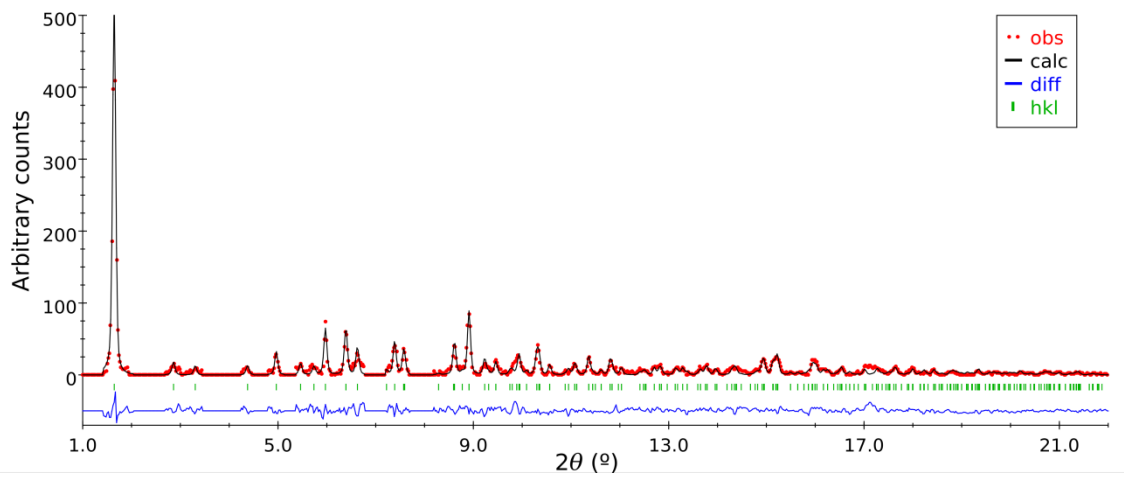


Fig. 6. Rietveld plot of brown aerinite. Top: Observed pattern with calculated one below. Bottom: Difference between observed and calculated patterns. The vertical markers show positions calculated for Bragg reflections.